The p75 neurotrophin receptor regulates proliferation of the MG63 osteoblastic cell line

Yuko Akiyama

Nihon University Graduate School of Dentistry,

Major in Orthodontics

(Directors : Profs. Noriyoshi Shimizu and Keitaro Isokawa,

and Assoc. Prof. Masaki Honda)

Contents

An article published as in the below and a new unpublished data on the assessment of mineralization in MG63 cell culture by alizarin red staining form the parts of this doctoral thesis:

> Akiyama Y, Mikami Y, Watanabe E, Watanabe N, Toriumi T, Takahashi T, Komiyama K, Isokawa K, Shimizu N, Honda MJ (2014) The p75 neurotrophin receptor regulates proliferation of the human MG63 osteoblast cell line. Differentiation (in press)

Abstract

The 75 kDa transmembrane protein, $p75^{NTR}$, is a marker of mesenchymal stem cells (MSCs). Isolated MSCs are capable of differentiating into osteoblasts, but the molecular function of $p75^{NTR}$ in MSCs and osteoblasts is poorly understood. The aim of this study was to examine the function of $p75^{NTR}$ in the human MG63 osteoblastic cell line compared to the murine MC3T3-E1 pre-osteoblast cell line.

MG63 cells and MC3T3-E1 cells expressing exogenous $p75^{NTR}$ protein (denoted as p75-MG63 and p75GFP-E1, respectively) were established to compare osteoblast differentiation and cell proliferation abilities. Overexpression of $p75^{NTR}$ induced higher alkaline phosphatase activity, mineralization capacity indicated by the positive staining with alizarin red and the mRNA expression of osteoblast-related genes such as osterix and bone sialoprotein in both p75-MG63 and p75GFP-E1. Interestingly, exogenous $p75^{NTR}$ stimulated cell proliferation and cell cycle progression in p75GFP-E1, but not in p75-MG63.

To elucidate any different effects of $p75^{NTR}$ expression on osteoblast differentiation and cell proliferation, mRNA expression of tropomyosin receptor kinase (trk) genes (trkA, trkB, trkC) and Nogo receptor (NgR) both of which are binding partners of $p75^{NTR}$ was examined by using real-time reverse transcription-polymerase chain reaction. Although trkA, trkB, and trkC were detected in both p75-MG63 and p75GFP-E1, NgR was detected only in p75-MG63. The signaling pathway for osteoblast differentiation and cell proliferation was identified by using the K252a inhibitor of the trks. Inhibition of trks by K252a suppressed $p75^{NTR}$-mediated osteoblast differentiation of p75GFP-E1, whereas deletion of the GDI domain in $P75^{NTR}$ from the p75-MG63 produced enhanced cell proliferation compared to p75-MG63.

These results suggest that $p75^{NTR}$ signaling associated with trk receptors promotes both cell proliferation and osteoblast differentiation, but that $p75^{NTR}$-mediated proliferation may be suppressed by signaling from the $p75^{NTR}$/NgR complex.

Introduction

Continuous remodeling in bone involves a balance between bone-forming osteoblasts derived from mesenchymal stem cells (MSCs) and bone-resorbing osteoclasts derived from hematopoietic stem cells. MSCs have been isolated from bone marrow, adipose tissue, umbilical cord, and dental-related tissues such as dental follicle, periodontal ligament, and dental pulp from adult and deciduous teeth (1-6). As a result, the strategy of engineering bone growth by using MSCs transplantation has become widely accepted (7). However, the proper utilization of MSCs/progenitors for clinical applications requires an integrated understanding of the molecular mechanisms involved in the differentiation from MSCs to osteoblasts.

Cell surface markers have been used for the selection of MSCs, but a single cell surface marker that exclusively defines MSCs has not been discovered (8). Recently, the 75 kDa transmembrane protein, $p75^{NTR}$, also referred to as nerve growth factor receptor (NGFR), tumor necrosis factor receptor superfamily member 16 (TNFRSF16), and CD271, has been described as a marker of MSCs in bone marrow, adipose tissue, and umbilical cord (9, 10). $p75^{NTR+}$ cells were isolated from deciduous dental pulp (DDP-$p75^{NTR+}$ cells) and those cells showed characteristics different from bone marrow-derived MSCs, which could differentiate into adipogenic and osteogenic lineages (11, 12). Although the differentiation of DDP-$p75^{NTR+}$ cells into osteoblasts and adipocytes was largely inhibited, a fraction of cells showed some such abilities (11). Interestingly, the presence of cells with the DDP-$p75^{NTR+}$ phenotype diminishes gradually with culture (11), a phenomenon also observed by others (13), and cells that had lost $p75^{NTR}$ expression were then capable of differentiating into osteoblasts and adipocytes (11). Furthermore, although DDP-$p75^{NTR+}$ cells showed high rates of proliferation in our hands, a slowly proliferating subpopulation of MSCs that highly expressed $p75^{NTR}$ was identified from umbilical cord blood (14). In contrast, $p75^{NTR+}$ cells were not found in human periodontal ligament-derived cells (6), and the use of $p75^{NTR}$ failed to isolate MSCs from umbilical cord blood (15). Taken together, these observations indicated that the properties of $p75^{NTR+}$ cells vary among different tissues or cells, which does not aid our understanding of the function of $p75^{NTR}$ in MSCs and osteoblasts.

A relationship between signalling from $p75^{NTR}$ and tropomyosin receptor

kinase (trk) has been documented in the nervous system (16, 17), but the function of $p75^{NTR}$ in MSCs and osteoblasts remains to be clarified. In this study, osteoblast differentiation of the murine C3H10T1/2 cells was inhibited by exogenous $p75^{NTR}$ expression. Interestingly, expression of the trk receptors (trk A, B and C) was not detected in the C3H10T1/2 cells, which suggests that trk signaling does not contribute to the $p75^{NTR}$-mediated inhibition of osteogblast differentiation (11). On the other hand, MC3T3-E1 pre-osteoblast cells constitutively expressing exogenous $p75^{NTR}$ show strongly enhanced cell proliferation and osteoblast differentiation (18). MC3T3-E1 cells express all of the trk receptors, and the osteoblast differentiation of MC3T3-E1 cells expressing exogenous p75 was inhibited by treatment with the K252a inhibitor of trk tyrosine kinase (18). These observations thus confirm that $p75^{NTR}$ signaling is associated with the trk tyrosine kinase receptor in MC3T3-E1 cells.

Mature osteoblast-like cells derived from the human MG63 osteoblastic cell line have been extensively studied in bone biology research. Comparisons of MC3T3-E1 cells with MG63 cells have revealed some phenotypic differences (19, 20); in particular, the cellular proliferation activities and osteoblast differentiation potential (19). Interestingly, the Nogo receptor, NgR, is expressed in MG63 cells, but not in MC3T3-E1 cells. The aim of this study was therefore to further examine the $p75^{NTR}$-mediated mechanisms of cell proliferation and osteoblast differentiation in MG63 cells compared to those operating in MC3T3-E1 cells containing exogenous $p75^{NTR}$.

Materials and Methods

1. Overexpression of $p75^{NTR}$

MG63 and MC3T3-E1 cells were obtained from the RIKEN cell bank (Ibaragi). $p75^{NTR}$ expression plasmids were constructed by standard methods. Human $p75^{NTR}$ and its deletion mutant cDNAs were prepared by polymerase chain reaction (PCR) and cloned into pIREShyg (Takara Bio, Tokyo). MG63 cells were plated at a density of 5×10^5 cells/well in a 6-well cell culture dish and cultured in α-MEM medium (Gibco BRL, Grand Island, NY, USA) with 10% fetal bovine serum (FBS, Japan Bioserum, Tokyo) and 1% penicillin-streptomycin (Gibco) for 24 h at 37°C in the presence of 5% CO_2. Subsequently, the cells were incubated in 2 mL of α-MEM containing 6.25 μL of lipofectamine LTX (Invitrogen, Carlsbad, CA, USA) and 2 μg of plasmid. The empty vector of IREShyg was used as a transfection control. Cells with stable DNA integration were selected by culturing with 200 mg/mL hygromycin (Sigma, St. Louis, MO, USA). Cells expressing $p75^{NTR}$ (p75-MG63) or mutant-$p75^{NTR}$ (p75Del-MG63) were selected from the transfected MG63 cells using the BD FACS Aria (BD Biosciences, San Jose, CA, USA) and a PE-conjugated human $p75^{NTR}$ antibody (BD Biosciences). MG63 cells stably transfected with empty expression vector (Mock-MG63) were similarly prepared and used as transfection control cells.

The stably transfected MC3T3-E1 cells expressing $p75^{NTR}$ fused to GFP (p75GFP-E1) and MC3T3-E1 cells expressing a non-fused GFP (GFP-E1) were established previously (18).

2. Cell culture and osteogenic induction protocol

Cells stably transfected with plasmid vector were grown to confluence in 12-well culture dishes in the growth medium at 37°C in the presence of 5% CO_2. Subsequently, the cells were subcultured for various periods in osteogenic induction medium containing α-MEM supplemented with 10% FBS, 50 μg/mL L-ascorbate phosphate (Sigma), 10 mM β-glycerophosphate (Sigma), and 100 ng/mL human recombinant bone morphogenetic protein-2 (hrBMP-2; R&D System, Minneapolis, MN, USA). Cells were maintained with fresh osteogenic induction medium every 2 days for the indicated period.

3. Observation by fluorescent microscopy

Cells were trypsinized and collected onto slides with a cytocentrifuge and fixed in 4% paraformaldehyde in phosphate-buffered saline (PBS) for 15 min at room temperature. The fixed cells were permeabilized in 0.5% NP-40 in PBS for 15 min at room temperature, and rinsed three times in PBS containing 0.5% bovine serum albumin. The p75-MG63 and Mock-MG63 cells were then incubated for 1 h at 37°C with PE-conjugated anti-human $p75^{NTR}$ antibody (BD Biosciences). The cells were then washed with PBS and the nuclei were counterstained with 0.2 μg/mL DAPI in Vectashield Antifade (Vector Laboratories, Burlingame, CA, USA). All immunofluorescence images were collected by fluorescence microscopy (Biozero BZ-8000, Keyence, Tokyo) and the images were analyzed with the Keyence software, BZ analyzer.

4. Cell counting assay

Cells were seeded onto 100-mm culture dishes (1×10^4 cells/dish) and cultured for the indicated periods in growth medium. The cells were then trypsinized and resuspended in growth media, and the number of cells was counted using a hemocytometer.

5. Cell cycle analysis

Cell cycle analysis was performed using Click-iT EdU Flow Cytometry Assay Kits (Invitrogen/Molecular Probes, Eugene, OR, USA) according to the manufacturer's instructions. In brief, cultured cells were treated with 10 μM EdU (5-ethynyl-2′-deoxyuridine) for 1 h. EdU is a nucleoside analog of thymidine and is incorporated into DNA during active DNA synthesis. The EdU-treated cells were fixed with paraformaldehyde for 15 min, washed once with PBS buffer containing bovine serum albumin, and then permeabilized with a saponin-based buffer for 30 min. The cells were then washed once, treated with the click-reaction mixture containing Pacific Blue azide for 30 min, washed once again, resuspended in PBS buffer, and analyzed on the BD FACS Aria.

6. Alkaline phosphatase staining

Cells were cultured in a 12-well cell culture dish under the previously described culture conditions before being rinsed twice and fixed in 4% paraformaldehyde in PBS (pH 7.3) for 15 min. Subsequently, cultures were

washed twice with PBS and incubated in alkaline phosphatase (ALP) substrated solution (pH 9.5) containing NBT/BCIP ready-to-use tablets (Roche Diagnostics, Penzberg, Germany). After a 15-min incubation, the cells were washed with distilled water, and examined using light microscopy and/or an EPSON GT-X800 scanner (Epson, Tokyo).

7. Alizarin red staining

Cells were cultured in a 12-well cell culture dish under the previously described culture conditions before being rinsed twice and fixed in 4% paraformaldehyde in 0.1 M cacodylate buffer (pH 7.3) for 30 min. Subsequently, cultures were washed with 0.1 M cacodylate buffer (pH 7.3), and stained for 5 min with a saturated solution of Alizarin Red-S (pH 4.0). The cells were washed with distilled water, then dried and examined using light microscopy and/or an EPSON GT-X800 scanner (Epson, Tokyo).

8. Real-time reverse transcription–PCR (real-time RT-PCR)

First-stranded cDNA was synthesized from 1 μg of DNase I-treated total RNA in a 20-μL reaction mixture containing 1× first-strand buffer, 50 ng of random primer, 10 mM dNTP mixture, 1 mM DTT, and 0.5 units of Super Script III RNase H^- reverse transcriptase (Invitrogen), which was incubated at 42°C for 1 h. Subsequently, the cDNA was diluted to 40 μL with sterile distilled water and a 2-μL aliquot of the diluted cDNA was subjected to real-time RT-PCR using SYBR Green I dye (Takara). The real-time RT-PCR was performed in a 25-μL reaction mixture containing 1× PCR buffer, 1.5 mM dNTP mixture, 1× SYBR Green I, 15 mM $MgCl_2$, 0.25 units of Ex Taq R-PCR (Takara), and 20 μM primers (sense and anti-sense; Table 1). Assays were performed on a Smart Cycler (Cepheid, Sunnyvale, CA, USA) and analyzed with the accompanying Smart Cycler software (Ver. 1.2d; Cepheid). Conditions for amplification were 40 cycles of 95°C for 3 s and 68°C for 20 s. Measurements commenced at the end of the annealing step (68°C).

9. RT-PCR

First-stranded cDNA was synthesized as described above. Mouse brain total RNA (Takara) was used as a positive control. A 2-μL aliquot of the synthesized cDNA solution was used for the PCR, which was performed on a

Smart Cycler (Cepheid). Conditions for amplification were 40 cycles of 95°C for 5 s and 68°C for 25 s. Subsequently, the PCR products were electrophoretically separated using a 2% agarose gel, stained with ethidium bromide, and photographed. The primer sets used for real time RT-PCR were listed in Table 2.

10. Statistical analysis

Results are presented as means ± SD of triplicate cultures and statistical differences were assessed using Student's *t*-test. Significant differences ($P < 0.05$) are indicated.

Results

1. Overexpression of $p75^{NTR}$ in MG-63 and MC3T3-E1 cells

In this study, human $p75^{NTR}$-expressing MG63 cells were established (p75-MG63) and they were used to investigate the effect of $p75^{NTR}$ on cell proliferation and osteoblast differentiation in comparison to MG63 cells stably transfected with the empty expression vector (Mock-MG63). The outcomes with forced expression of $p75^{NTR}$ in p75-MG63 were compared with those for MC3T3-E1 which was stably expressing mouse $p75^{NTR}$ fused with GFP (p75GFP-E1).

RT-PCR analysis revealed the elevated levels of $p75^{NTR}$ mRNA in p75-MG63 and p75GFP-E1, and slightly elevated levels in GFP-E1 and Mock-MG63 (Fig. 1A). Immunofluorescence microscopy showed the protein localization of $p75^{NTR}$ in the cell membrane of p75-MG63 and p75GFP-E1, but $p75^{NTR}$ protein was only slightly detected in Mock-MG63 and GFP-E1 cell membrane (Fig. 1B). No morphological difference was observed by phase contrast microscopy between p75-MG63 and Mock-MG63, or between p75GFP-E1 and GFP-E1 during the growth phase (Fig. 1C).

2. Cell proliferation and cell cycle progression

The effect of $p75^{NTR}$ on cell proliferation was determined after 6 d in culture. Although p75GFP-E1 proliferated more rapidly than GFP-E1, there was no significant difference between the p75-MG63 and Mock-MG63 (Fig. 2A). An analysis of cell cycle progression showed that more p75GFP-E1 than GFP-E1 entered S-phase, although there was no significant difference in the number of cells entering S-phase between p75-MG63 and Mock-MG63 (Fig. 2B).

3. Osteoblast differentiation

To determine whether $p75^{NTR}$ expression affected the osteoblast differentiation of MG63 cells, ALP activity in p75-MG63 and Mock-MG63 was compared with that in p75GFP-E1 and GFP-E1. The results of alizarin red staining were also compared between p75-MG63 and Mock-MG63 under osteogenic induction at the indicated time point. After 3 d of induction, both p75-MG63 and p75GFP-E1 showed more intense ALP staining than each mock

cell line (Fig. 3A). Mineralized nodules were observed in p75-MG63 culture after 12 days and the time course observations revealed that $p75^{NTR}$ have promoted mineralization as clearly shown by alizarin red staining (Fig. 3B).

The effect of $p75^{NTR}$ on osteoblast differentiation was examined by real-time RT-PCR measurements of the mRNA expression of osteoblast transcription factors, Runx2 and OSX, as well as osteoblast markers such as bone sialoprotein (BSP) and osteocalcin (OC) (Fig. 3C). No difference was observed in the mRNA expression levels of Runx2, OSX, BSP and OC between $p75^{NTR}$ expressing cells and mock cells in MG63 cells and MC3T3-E1 at day 3, which is the early phase of differentiation. In contrast, the mRNA levels of OSX and BSP increased in p75-MG63 and p75GFP-E1 compared to the mock cells during the late phase of differentiation by day 12. OC mRNA expression also increased in p75GFP-E1 compared to GFP-E1, but there was no significant difference in Runx2 expression among all the cells tested.

4. Signaling pathway regulating $p75^{NTR}$-mediated osteoblast differentiation

$p75^{NTR}$ participates in two signaling pathways; one involves heterodimer formation with trk receptors and the other involves heterodimerization with the NgR. Heterodimerization of $p75^{NTR}$ with trk receptors activates tyrosine kinase activity, whereas heterodimerization with NgR activates GTP kinase via RhoA. The relative involvement of each pathway was assayed by measuring the mRNA expression of trk receptor family members and of NgR in all cell lines. Interestingly, the expression of trkA, B and C mRNAs was detectable in all cell lines, but NgR mRNA was detected only in p75-MG63 and Mock-MG63 (Fig. 4).

It has been previously reported that the proliferation and osteoblast differentiation potentials of p75GFP-E1 are induced via the trk signaling pathway, but not via the NgR signaling pathway (18). To further elucidate whether RhoA-GTP kinase signaling was involved in the $p75^{NTR}$-mediated osteoblast differentiation in MG63 cells, a $p75^{NTR}$-deleted mutant cell line (p75Del-MG63) that stably expresses a mutant $p75^{NTR}$ protein with the GDI-binding domain deleted was established (Fig. 5A). The p75Del-MG63 and Mock-MG63 were cultured with osteogenic induction medium for 12 d, and ALP staining as well as real-time RT-PCR were performed. The p75Del-MG63 showed a higher ALP activitys compared with Mock-MG63 cells (Fig. 5B). Similarly, the expression of both OSX and BSP mRNAs increased in p75Del-MG63 compared with Mock-MG63 (Fig. 5C). These results were consistent with those obtained from a

comparison between p75-MG63 and Mock-MG63. The p75Del-MG63 also showed considerably greater cell proliferation than Mock-MG63 after culturing for 3 d (Fig. 5D), and FACS analysis of cell cycle progression confirmed a greater number of cells entering S-phase for p75Del-MG63 than for Mock-MG63 (Fig. 5E).

Discussion

The $p75^{NTR}$ protein is an important neuronal signaling molecule that interacts with numerous ligands and co-receptors (17, 21). Recently, $p75^{NTR}$ protein expression has been used as a marker to isolate MSCs, and the $p75^{NTR+}$ cells are considered to be capable of differentiating into osteoblasts (12, 22). The mineralization capacity of $p75^{NTR}$-expressing cells, which are derived from human periosteum was found to be higher than periosteum-derived $p75^{NTR}$ negative cells (23). It was reported previously that exogenous $p75^{NTR}$ enhances the potential for both osteoblast differentiation and cell proliferation in the pre-osteoblast MC3T3-E1 (18). The present study confirms that $p75^{NTR}$ plays a role in osteoblast differentiation because $p75^{NTR}$ overexpression is also associated with enhanced ALP activity and mRNA expression of osteogenic differentiation marker genes in the MG63 osteoblastic cell line.

Runx2 is one of the master genes that regulates osteoblast differentiation through inducing transcription of the BSP and OC osteoblast marker genes (24, 25). In the present study, there was no difference in Runx2 expression between exogenous $p75^{NTR}$-expressing cells and the MOCK control cell lines during the culture period. The expression of OSX is required for osteoblast differentiation (26) and OSX expression was dependent upon $p75^{NTR}$ expression at day 12 in both cell types. This suggests that $p75^{NTR}$ induces osteoblast differentiation via OSX during the late phase of differentiation.

$p75^{NTR}$ has dual roles in signaling for both neurotrophins and myelin-associated glycoprotein (MAG) (27). Neurotrophins binding to $p75^{NTR}$ and promote axonal outgrowth of neurons presumably by inhibiting RhoA activity (28), whereas MAG elicits the opposite effect via $p75^{NTR}$ on neurons by activating RhoA (27). The expression of all trk receptors (trkA, B and C) was detected in both p75-MG63 and p75GFP-E1, which is consistent with previous observations that trk receptors are expressed in MC3T3-E1 (29, 30). Furthermore, a pharmacological study using K252a, an inhibitor of trk tyrosine kinase suppressed $p75^{NTR}$-mediated osteoblast differentiation of MC3T3-E1 (Supplemental data). These observations indicate that $p75^{NTR}$ activates a tyrosine kinase signaling pathway (21, 31). K252a inhibits JNK and promotes cell survival by activating ERK1/2 and Akt (32). JNK is associated with $p75^{NTR}$ activation and the induction of cell death (16, 33). Therefore, $p75^{NTR}$ may

regulate the expression of the osteoblast marker genes, OSX, BSP and OC involving JNK in p75-MG63 and p75GFP-E1, via a novel link between JNKs and trk receptors.

The neurotrophin/trk receptor autocrine signaling pathway is required for the survival of proliferating human osteoblasts (33), and $p75^{NTR}$ stimulates proliferation of hepatic stellate cells (34). It is shown in this study that overexpression of $p75^{NTR}$ enhances the proliferation and cell cycle progression of p75GFP-E1. In contrast, $p75^{NTR}$ overexpression did not mediate the proliferation of p75-MG63. Previous reports have demonstrated that $p75^{NTR}$ interacts with the NgR to inhibit neurite outgrowth (35, 36), which is mediated by the release of RhoA from the intracellular regulator of the cytoskeleton, Rho-GDI (27, 36-38). NgR expression in p75GFP-E1 and p75-MG63 was examined to clarify the different effect of $p75^{NTR}$ on cell proliferation between these cells. NgR is expressed in p75-MG63, but not in p75GFP-E1 and therefore it could be plausible that a $p75^{NTR}$-NgR complex has a role in activating the RhoA/Rho kinase pathway.

To investigate this hypothesis, MG63 cell line which is stably expressing GDI binding domain–lacking $p75^{NTR}$ was established (p75Del-MG63) and cultured for 12 d in osteogenic induction medium. ALP activity and the expression of osteoblast marker genes in p75Del-MG63 were not significantly different from p75-MG63. In contrast, cell proliferation and cell cycle progression were strongly enhanced in p75Del-MG63, when compared to Mock-MG63 and p75-MG63. These results indicate that $p75^{NTR}$ regulates the cell proliferation in NgR-expressing MG63 osteoblastic cell line via the RhoA/Rho kinase pathway. Rho-associated protein kinases (ROCKs) are downstream effector proteins of RhoA (39), and activation of the Rho/ROCK pathway induces both apoptosis and non-apoptotic cell death (40, 41). In addition, a specific ROCK1 and ROCK2 inhibitor, Y27632, enhances the proliferation of embryonic stem cells and induced pluripotent stem cells (39, 42, 43). Activation of RhoA-ROCK signaling by $p75^{NTR}$ may suppress $p75^{NTR}$-trk stimulation of MG63 cells proliferation.

Conclusion

MG63 cells and MC3T3-E1 cells overexpressing exogenous $p75^{NTR}$ were established to explore its functions in cell proliferation and osteoblast differentiation. Results demonstrated in this study suggest that $p75^{NTR}$ signaling associated with trk receptors promotes both cell proliferation and osteoblast differentiation, but $p75^{NTR}$-mediated proliferation may be suppressed by $p75^{NTR}$ /NgR signaling pathway.

Acknowledgments

I am grateful to Profs. Noriyoshi Shimizu, Masao Maeno and Keitaro Isokawa, and Assoc. Prof. Masaki Honda for their valuable suggestions and critical reading, and to all the colleagues in the Departments of Orthodontics and Anatomy for their technical assistance and continuous encouragement. This doctoral work was supported by Grant from Dental Research Center, Nihon University School of Dentistry for 2011, 2012 and 2013 to YA, and supported in part by Grants-in-Aid for Scientific Research (B) (21390528 and 24390447) to MH and grants from the Dental Research Center to MH and YM, and Sato Fund, Nihon University School of Dentistry, and Nihon University Multidisciplinary Research Grant for 2012 and 2013 to MH.

References

1) Pittenger MF, Mackay AM, Beck SC, Jaiswal RK, Douglas R, Mosca JD, Moorman MA, Simonetti DW, Craig S, Marshak DR (1999) Multilineage potential of adult human mesenchymal stem cells. Science 284, 143-147.

2) Gronthos S, Mankani M, Brahim J, Robey PG, Shi S (2000) Postnatal human dental pulp stem cells (DPSCs) in vitro and in vivo. Proc Natl Acad Sci U S A 97, 13625-13630.

3) Seo BM, Miura M, Gronthos S, Bartold PM, Batouli S, Brahim J, Young M, Robey PG, Wang CY, Shi S (2004) Investigation of multipotent postnatal stem cells from human periodontal ligament. Lancet 364, 149-155.

4) Honda MJ, Nakashima F, Satomura K, Shinohara Y, Tsuchiya S, Watanabe N, Ueda M (2007) Side population cells expressing ABCG2 in human adult dental pulp tissue. Int Endod J 40, 949-958.

5) Honda MJ, Imaizumi M, Tsuchiya S, Morsczeck C (2010) Dental follicle stem cells and tissue engineering. J Oral Sci 52, 541-552.

6) Honda MJ, Imaizumi M, Suzuki H, Ohshima S, Tsuchiya S, Satomura K (2011) Stem cells isolated from human dental follicles have osteogenic potential. Oral Surg Oral Med Oral Pathol Oral Radiol Endod 111, 700-708.

7) Ishikane S, Hosoda H, Yamahara K, Akitake Y, Kyoungsook J, Mishima K, Iwasaki K., Fujiwara M, Miyazato M, Kangawa K, Ikeda T (2013) Allogeneic transplantation of fetal membrane-derived mesenchymal stem cell sheets increases neovascularization and improves cardiac function after myocardial infarction in rats. Transplantation 96, 697-706.

8) Barry FP, Murphy JM (2004) Mesenchymal stem cells: clinical applications and biological characterization. Int J Biochem Cell Biol 36, 568-584.

9) Dmitrieva RI, Minullina IR, Bilibina AA, Tarasova OV, Anisimov SV, Zaritskey AY (2012) Bone marrow- and subcutaneous adipose tissue-derived mesenchymal stem cells: differences and similarities. Cell cycle 11, 377-383.

10) Christodoulou I, Kolisis FN, Papaevangeliou D, Zoumpourlis V (2013) Comparative evaluation of human mesenchymal stem cells of fetal (Wharton's

jelly) and adult (adipose tissue) origin during prolonged *in vitro* expansion: considerations for cytotherapy. Stem Cells Int 2013, 246134.

11) Mikami Y, Ishii Y, Watanabe N, Shirakawa T, Suzuki S, Irie S, Isokawa K, Honda MJ (2011) CD271/p75^{NTR} inhibits the differentiation of mesenchymal stem cells into osteogenic, adipogenic, chondrogenic, and myogenic lineages. Stem Cells Dev 20, 901-913.

12) Quirici N, Soligo D, Bossolasco P, Servida F, Lumini C, Deliliers GL (2002) Isolation of bone marrow mesenchymal stem cells by anti-nerve growth factor receptor antibodies. Exp Hematol 30, 783-791.

13) Margossian T, Reppel L, Makdissy N, Stoltz JF, Bensoussan D, Huselstein C (2012) Mesenchymal stem cells derived from Wharton's jelly: comparative phenotype analysis between tissue and in vitro expansion. Biomed Mater Eng 22, 243-254.

14) Ju XA, Chen J, Ding L, Li YZ, Xiao FJ, Li ZQ, Guo ZK (2013) A slowly proliferating subpopulation in human umbilical cord mesenchymal stem cells in culture. In Vitro Cell Dev Biol Anim 49, 653-656.

15) Watson JT, Foo T, Wu J, Moed BR, Thorpe M, Schon L, Zhang Z (2013) CD271 as a marker for mesenchymal stem cells in bone marrow versus umbilical cord blood. Cells Tissues Organs 197, 496-504.

16) Kaplan DR, Miller FD (2000) Neurotrophin signal transduction in the nervous system. Curr Opin Neurobiol 10, 381-391.

17) Patapoutian A, Reichardt LF (2001) Trk receptors: mediators of neurotrophin action. Curr Opin Neurobiol 11, 272-280.

18) Mikami Y, Suzuki S, Ishii Y, Watanabe N, Takahashi T, Isokawa K, Honda MJ (2012) The p75 neurotrophin receptor regulates MC3T3-E1 osteoblastic differentiation. Differentiation 84, 392-399.

19) Czekanska EM, Stoddart MJ, Ralphs JR, Richards RG, Hayes JS (2013) A phenotypic comparison of osteoblast cell lines versus human primary osteoblasts for biomaterials testing. J Biomed Mater Res A 24, a34937.

20) Miron RJ, Caluseru OM, Guillemette V, Zhang Y, Gemperli AC, Chandad F, Sculean, A (2013) Influence of enamel matrix derivative on cells at different maturation stages of differentiation. PLoS One 8, e71008.

21) Mischel PS, Smith SG, Vining ER, Valletta JS, Mobley WC, Reichardt LF (2001) The extracellular domain of $p75^{NTR}$ is necessary to inhibit neurotrophin-3 signaling through TrkA. J Biol Chem 276, 11294-11301.

22) Battula VL, Treml S, Bareiss PM, Gieseke F, Roelofs H, de Zwart P, Muller I, Schewe B, Skutella T, Fibbe WE, Kanz L, Buhring HJ (2009) Isolation of functionally distinct mesenchymal stem cell subsets using antibodies against CD56, CD271, and mesenchymal stem cell antigen-1. Haematologica 94, 173-184.

23) Alexander D, Schafer F, Munz A, Friedrich B, Klein C, Hoffmann J, Buhring HJ, Reinert S (2009) LNGFR induction during osteogenesis of human jaw periosteum-derived cells. Cell Physiol Biochem 24, 283-290.

24) Ducy P, Zhang R, Geoffroy V, Ridall AL, Karsenty G (1997) Osf2/Cbfa1: a transcriptional activator of osteoblast differentiation. Cell 89, 747-754.

25) Ducy P (2000) Cbfa1: a molecular switch in osteoblast biology. Dev Dyn 219, 461-471.

26) Nakashima K, Zhou X, Kunkel G, Zhang Z, Deng JM, Behringer RR, de Crombrugghe B (2002) The novel zinc finger-containing transcription factor osterix is required for osteoblast differentiation and bone formation. Cell 108, 17-29.

27) Yamashita T, Higuchi H, Tohyama M (2002) The p75 receptor transduces the signal from myelin-associated glycoprotein to Rho. J Cell Biol 157, 565-570.

28) Yamashita T, Tucker KL, Barde YA (1999) Neurotrophin binding to the p75 receptor modulates Rho activity and axonal outgrowth. Neuron 24, 585-593.

29) Mogi M, Kondo A, Kinpara K, Togari A (2000) Anti-apoptotic action of nerve growth factor in mouse osteoblastic cell line. Life Sci 67, 1197-1206.

30) Nakanishi T, Ohyama K, Aoki C, Kudo A, Hattori T, Takahashi K, Taniguchi S, Takigawa M (1994) Expression of trkC in a mouse osteoblastic cell line and its response to neurotrophin-3. Biochem Biophys Res Commun 203, 1268-1274.

31) Rodriguez-Tebar A, Dechant G, Gotz R, Barde YA (1992) Binding of neurotrophin-3 to its neuronal receptors and interactions with nerve growth factor and brain-derived neurotrophic factor. EMBO J 11, 917-922.

32) Koizumi S, Contreras ML, Matsuda Y, Hama T, Lazarovici P, Guroff G (1988) K-252a: a specific inhibitor of the action of nerve growth factor on PC 12 cells. J Neurosci 8, 715-721.

33) Roux PP, Barker PA (2002) Neurotrophin signaling through the p75 neurotrophin receptor. Prog Neurobiol 67, 203-233.

34) Asai K, Tamakawa S, Yamamoto M, Yoshie M, Tokusashi Y, Yaginuma Y, Kasai S, Ogawa K (2006) Activated hepatic stellate cells overexpress p75NTR after partial hepatectomy and undergo apoptosis on nerve growth factor stimulation. Liver Int 26, 595-603.

35) Wang KC, Kim JA, Sivasankaran R, Segal R, He Z (2002) p75 interacts with the Nogo receptor as a co-receptor for Nogo, MAG and OMgp. Nature 420, 74-78.

36) Wong ST, Henley JR, Kanning KC, Huang KH, Bothwell M, Poo MM (2002) A $p75^{NTR}$ and Nogo receptor complex mediates repulsive signaling by myelin-associated glycoprotein. Nat Neurosci 5, 1302-1308.

37) Yamashita T, Tohyama M (2003) The p75 receptor acts as a displacement factor that releases Rho from Rho-GDI. Nat Neurosci 6, 461-467.

38) Al Halabiah H, Delezoide AL, Cardona A, Moalic JM, Simonneau M (2005) Expression pattern of NOGO and NgR genes during human development. Gene Expr Patterns 5, 561-568.

39) Horani A, Nath A, Wasserman MG, Huang T, Brody SL (2013) Rho-associated protein kinase inhibition enhances airway epithelial Basal-cell proliferation and lentivirus transduction. Am J Respir Cell Mol Biol 49, 341-347.

40) Wen HC, Kao C, Hsu RC, Huo YN, Ting PC, Chen LC, Hsu SP, Juan SH, Lee WS (2013) Thy-1-induced migration inhibition in vascular endothelial cells through reducing the RhoA activity. PLoS One 8, e61506.

41) Chang J, Xie M, Shah VR, Schneider MD, Entman ML, Wei L, Schwartz RJ (2006) Activation of Rho-associated coiled-coil protein kinase 1 (ROCK-1) by caspase-3 cleavage plays an essential role in cardiac myocyte apoptosis. Proc Natl Acad Sci U S A 103, 14495-14500.

42) Watanabe K, Ueno M, Kamiya D, Nishiyama A, Matsumura M, Wataya T, Takahashi JB, Nishikawa S, Nishikawa S, Muguruma K, Sasai Y (2007) A

ROCK inhibitor permits survival of dissociated human embryonic stem cells. Nat Biotechnol 25, 681-686.

43) Liu X, Ory V, Chapman S, Yuan H, Albanese C, Kallakury B, Timofeeva OA, Nealon C, Dakic A, Simic V, Haddad BR, Rhim JS, Dritschilo A, Riegel A, McBride A, Schlegel R (2012) ROCK inhibitor and feeder cells induce the conditional reprogramming of epithelial cells. Am J Pathol 180, 599-607.

Table 1. PCR primer used in real time RT-PCR

Targets		Primer sequence	Genbank Acc No.
hRunx2	Forward	5'-CACAAATCCTCCCCAAGTAG-3'	NM_001015051.3
	Reverse	5'-GGAGGGCCGTGGGTTCTGAG-3'	
mRunx2	Forward	5'-ACA ACCACAGAACCACAAG-3'	NM_001145920.2
	Reverse	5'-TCT CGGTGGCTGGTAGTGA-3'	
hOSX	Forward	5'-GCCAGAAGCTGTGAAACCTC-3'	NM_001173467.1
	Reverse	5'-GCTGCAAGCTCTCCATAACC-3'	
mOSX	Forward	5'-GGA GGTTTCACTCCATTCCA-3'	NM_130458.3
	Reverse	5'-TAG AAGGAGCAGGGGACAGA-3'	
hBSP	Forward	5'-AGGGCAGTAGTGACTC-3'	NM_004967.3
	Reverse	5'-AGCCCAGTGTTGTAGC-3'	
mBSP	Forward	5'-TGA AACGGTTTCCAGTCCAG-3'	NM_008318.3
	Reverse	5'-TGG TCTTCATTCCCCTCAG-3'	
hOC	Forward	5'-AGGGCAGCGAGGTAGTGAAG-3'	NM_199173.4
	Reverse	5'-AAGGGCAAGGGGAAGAGGAAAG-3'	
mOC	Forward	5'-GAC AAGTCCCACACAGCAGC-3'	NM_031368.4
	Reverse	5'-GGA CATGAAGGCTTTGTCAG-3'	
hb-actin	Forward	5'-TTCCAGCCTTCCTTCCTGG-3'	NM_001101.3
	Reverse	5'-TTGCGCTCAGGAGGAGCAA-3'	
mb-actin	Forward	5'-CTT TCTACAATGAGCTGCGTG-3'	NM_007393.3
	Reverse	5'-ATG GCTGGGGTGTTGAAGG-3'	

Table 2. PCR primer used in RT-PCR

Targets		Primer sequence	Genbank Acc No.
hp75^{NTR}	Forward	5'-TTGTGGCCTACATAGCCTTCAAGA-	NM_002507.3
	Reverse	5'-TCCACGGAGATGCCACTGTC-3'	
mp75^{NTR}	Forward	5'-TTG	NM_033217.3
	Reverse	5'-TCC ACAGAGATGCCGCTGTC-3'	
hTrkA	Forward	5'-TCACCAGTGACCTCAACAG-3'	NM_001007792.1
	Reverse	5'-CAGAGACGGTGCCGGCTGC-3'	
mTrkA	Forward	5'-ATG TGACGTGCTGGGCAG-3'	NM_001033124.1
	Reverse	5'-AGA GACGGTGCTGGCTGC-3'	
hTrkB	Forward	5'-GTACTGCCTGAATGAAAGC-3'	NM_001007097.1
	Reverse	5'-CACCTGCCACACTACAG-3'	
mTrkB	Forward	5'-GTT CACGTGCTCCTGCGAC-3'	NM_001025074.2
	Reverse	5'-CTT TCCTTCCTCCACGGTG-3'	
hTrkC	Forward	5'-TGCGTTATATAAACCTGTC-3'	NM_001007156.2
	Reverse	5'- AGCGTTGATGCAGTAGAG-3'	
mTrkC	Forward	5'-GCT GAGCCTTCGGGAATTG-3'	NM_008746.5
	Reverse	5'-CAC TGATCTCTGGGAGATC-3'	
hNgR	Forward	5'-AACCCCTACGATGAAGAG-3'	NM_023004.5
	Reverse	5'-CAGGATGGTGAGGTTGCG-3'	
mNgR	Forward	5'-GAC CCCGAAGATGAAGAG-3'	NM_022982.2
	Reverse	5'-CAG GATAGTGAGATTTCG-3'	
hb-actin	Forward	5'-TTCCAGCCTTCCTTCCTGG-3'	NM_001101.3
	Reverse	5'-TTGCGCTCAGGAGGAGCAA-3'	
mb-actin	Forward	5'-CTT TCTACAATGAGCTGCGTG-3'	NM_007393.3
	Reverse	5'-ATG GCTGGGGTGTTGAAGG-3'	

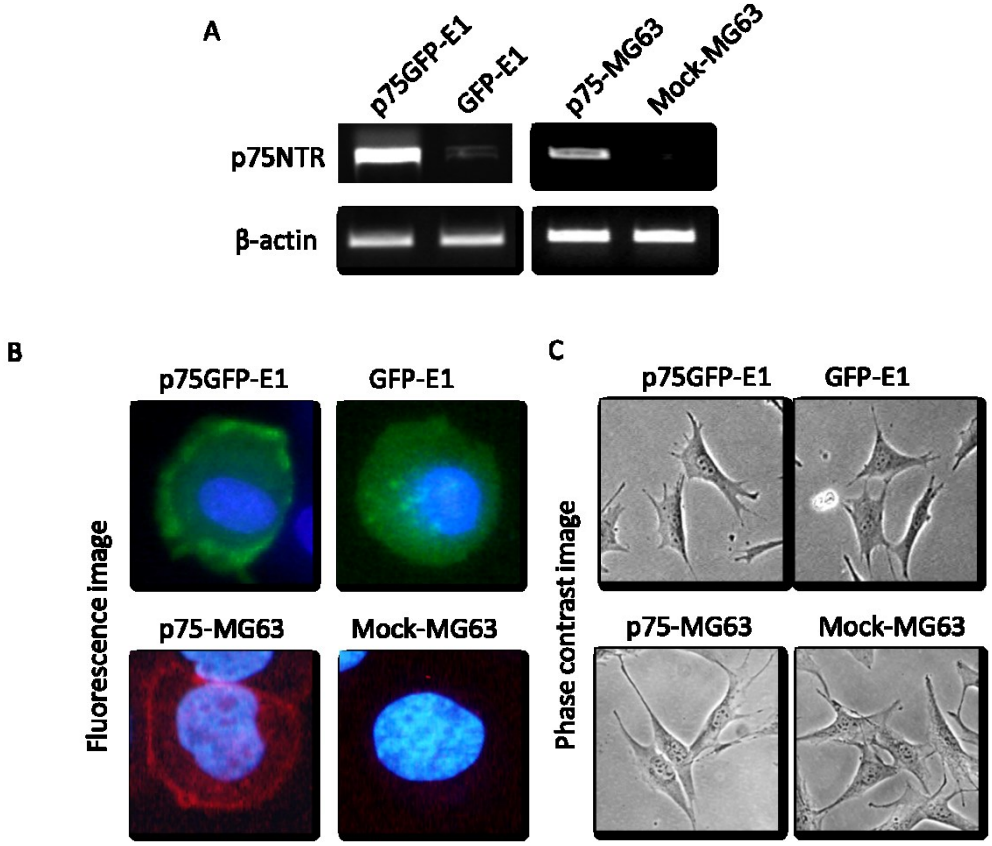

Fig. 1. Overexpression of $p75^{NTR}$-GFP in MC3T3-E1 cells and $p75^{NTR}$ in MG63 cells.

(A) $p75^{NTR}$ or/and $p75^{NTR}$-GFP mRNA expression. Cells were cultured in growth medium until confluence, and mRNA expression level of $p75^{NTR}$ or/and $p75^{NTR}$-GFP was measured by RT-PCR. ß-actin mRNA was measured as an internal control.

(B) Localization of $p75^{NTR}$-GFP in MC3T3-E1 cells and $p75^{NTR}$ in MG63 cells. GFP signals in p75GFP-E1 and GFP-E1 are in green. p75-MG63 and Mock-MG63 were immunocytochemically stained with PE-conjugated anti-human $p75^{NTR}$ antibody. The PE signals are in red and DNA/nucleus stained with DAPI in blue. Representative immunofluorescence images are shown.

(C) Cell morphology observed by phase-contrast microscopy.

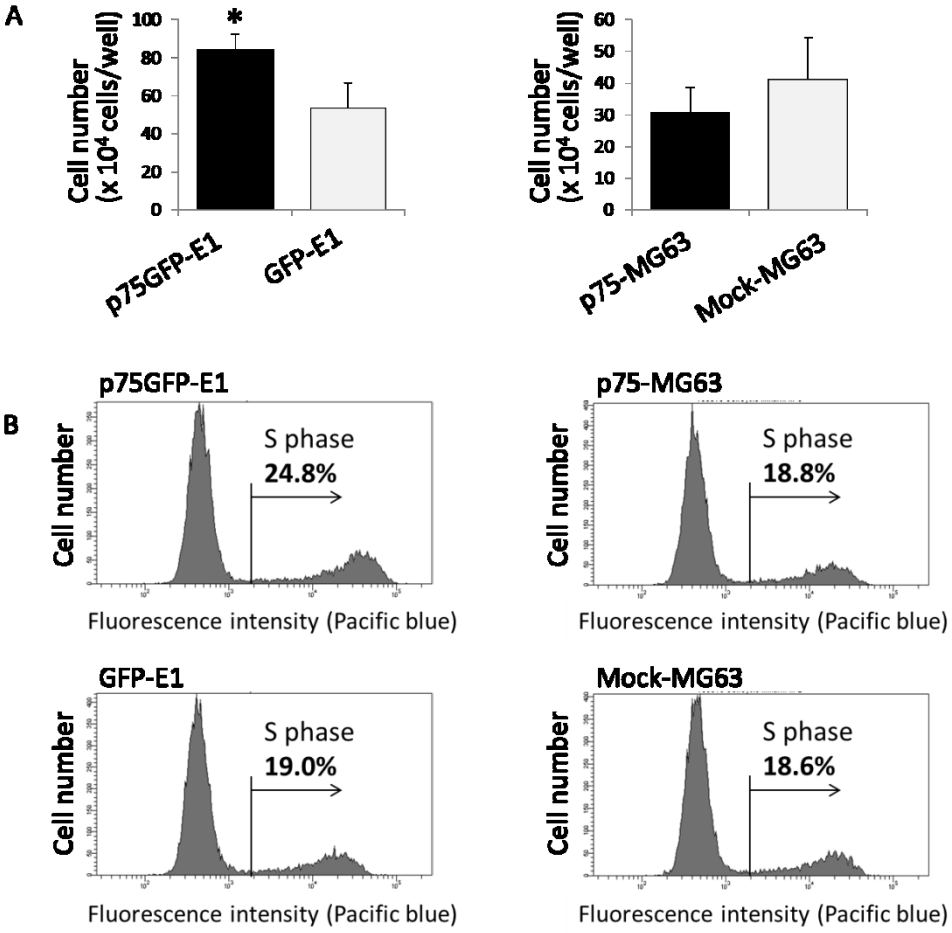

Fig. 2. Effect of $p75^{NTR}$ overexpression on cell proliferation and cell cycle progression.

(A) Cells were cultured in growth medium for 3 d and the cell numbers were counted to assess proliferation. Mean ± S.D. (n = 3) $*P < 0.05$ compared with mock cells.

(B) Cells in a logarithmic growth phase were treated with EdU for 1 h. EdU-incorporated cells were labeled with Pacific Blue™ azide and cell cycle progression was assessed by FACS analysis using a 407-nm excitation and 450/50-nm bandpass filter.

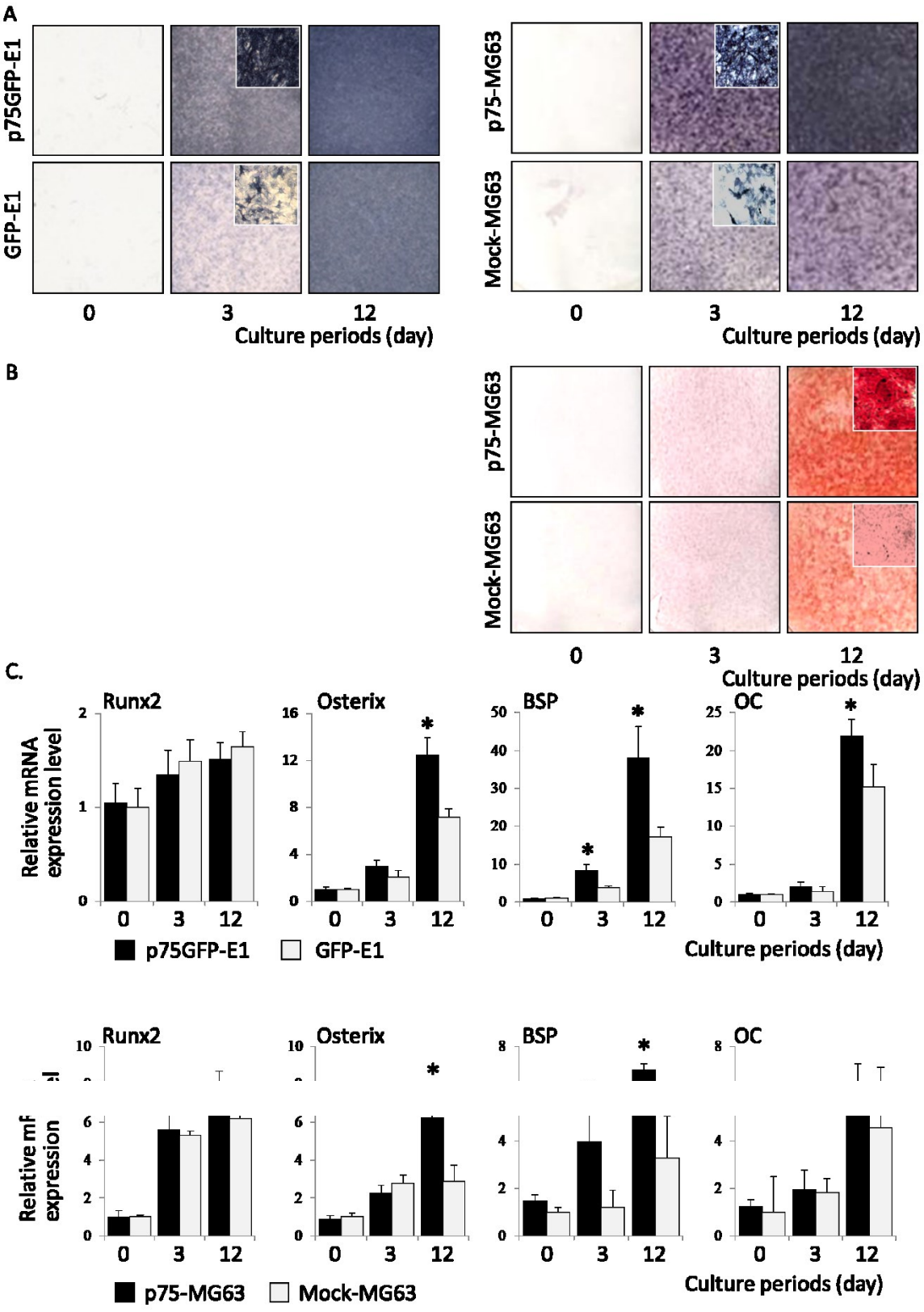
A
p75GFP-E1
GFP-E1
p75-MG63
Mock-MG63
0
3
12
Culture periods (day)
B
C.
Runx2
Osterix
BSP
OC
Relative mRNA expression level
p75GFP-E1
GFP-E1
p75-MG63
Mock-MG63

Fig. 3. Effect of $p75^{NTR}$ overexpression on osteoblast differentiation.

(A) Cells were cultured in growth medium until confluence, and then switched to osteogenic induction medium for the indicated number of days before ALP staining. The images of stained cultures were obtained using an EPSON scanner, GT-X800. The stained cultures on day 3 were also observed by phase-contrast microscopy (insets).

(B) Cells were cultured in growth medium until confluence, and then switched to osteogenic induction medium for the indicated number of days before alizarin red staining. The stained cultures on day 3 were also observed by phase-contrast microscopy (insets).

(C) mRNA expression levels of osteoblast differentiation-related genes were assessed in the cells cultured in osteogenic induction medium as shown in (A), using real-time RT-PCR. Data represent the mean ± S.D. (n = 3). $*P < 0.05$ compared with mock cells at each time point.

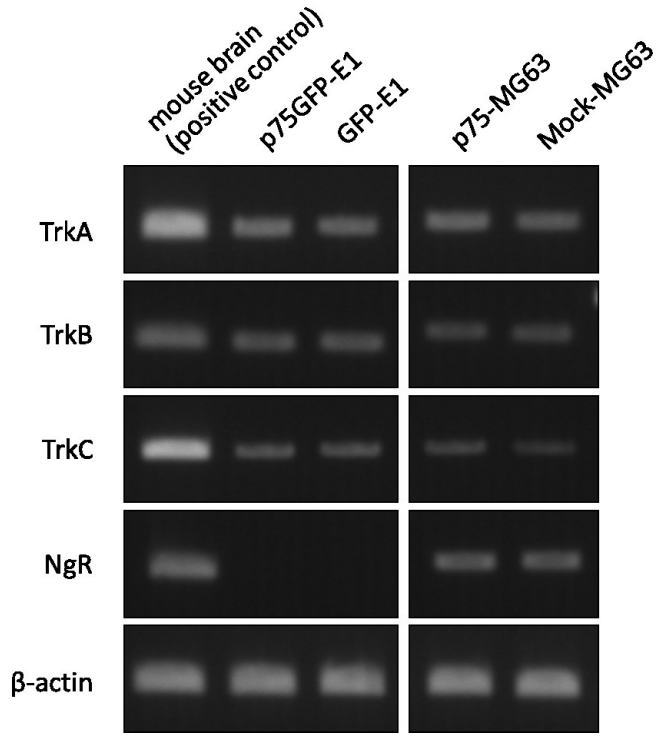

Fig. 4. mRNA expression of Trks and NgR genes.

Cells were cultured in growth medium until confluence, and then switched to osteogenic induction medium for 12 d before the mRNA was extracted. RT-PCR was used to measure the mRNA expressions of TrkA, TrkB, TrkC and NgR. β-actin mRNA expression was measured as an internal control. Mouse brain was analyzed as a positive control.

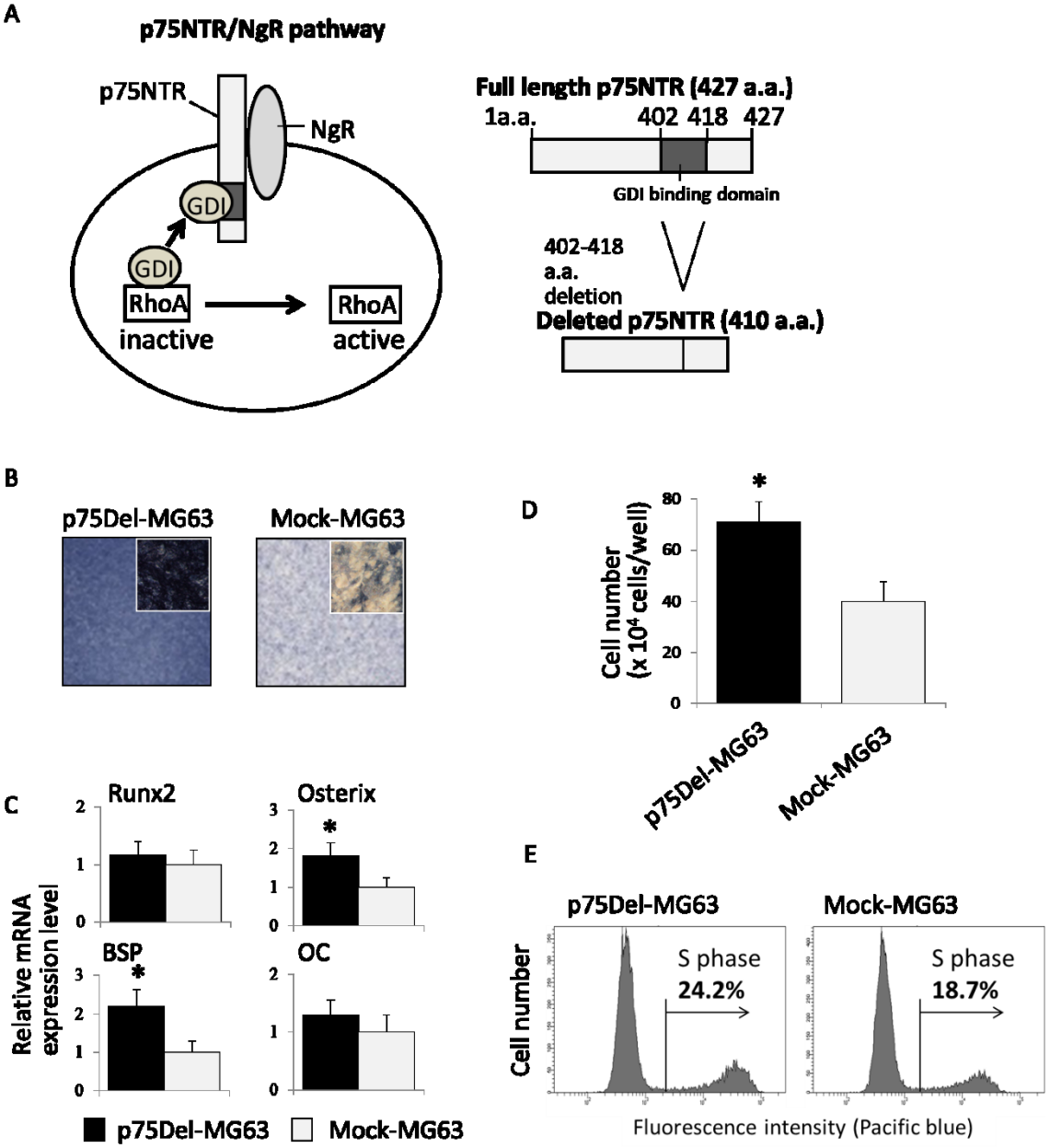
A
p75NTR/NgR pathway
p75NTR
NgR
GDI
GDI
RhoA
inactive
RhoA
active
Full length p75NTR (427 a.a.)
1a.a.
402 418 427
GDI binding domain
402-418
a.a.
deletion
Deleted p75NTR (410 a.a.)
B
p75Del-MG63
Mock-MG63
C
Runx2
Osterix
BSP
OC
Relative mRNA expression level
p75Del-MG63
Mock-MG63
D
Cell number (x 10⁴ cells/well)
p75Del-MG63
Mock-MG63
E
p75Del-MG63
Mock-MG63
Cell number
S phase
24.2%
S phase
18.7%
Fluorescence intensity (Pacific blue)

Fig. 5. Effect of deleting the GDI-binding domain on osteoblast differentiation and proliferation in MG63 cells.

(A) Schema illustrating the $p75^{NTR}$/NgR signaling pathway and deletion of GDI-binding domain in the $p75^{NTR}$ mutant.

(B) Cells were cultured in growth medium until confluence, and then switched to osteogenic induction medium for 12 d before ALP staining. The images of stained cultures were obtained using a scanner and by phase-contrast microscopy (insets).

(C) mRNA expression levels of Runx2, OSX, BSP and OC in the cells cultured in osteogenic induction medium were measured as described in (D). After culture, real-time RT-PCR was conducted.

(D) To assess the effect of deleting the GDI-binding domain on cell proliferation, cells were cultured in growth medium for 3 d, and then the cell numbers were counted. Mean ± S.D. (n = 3), * $P <$ 0.05 compared with the corresponding mock cells.

(E) To assess cell cycle progression, cells in logarithmic growth phase were treated with EdU for 1 h. EdU-incorporated cells were labeled by Pacific Blue™ azide and then they were detected by FACS analysis using a 407-nm excitation and 450/50-nm bandpass filter. Data represent the mean ± S.D. (n = 3). * $P < 0.05$ compared with mock cells at each time point.

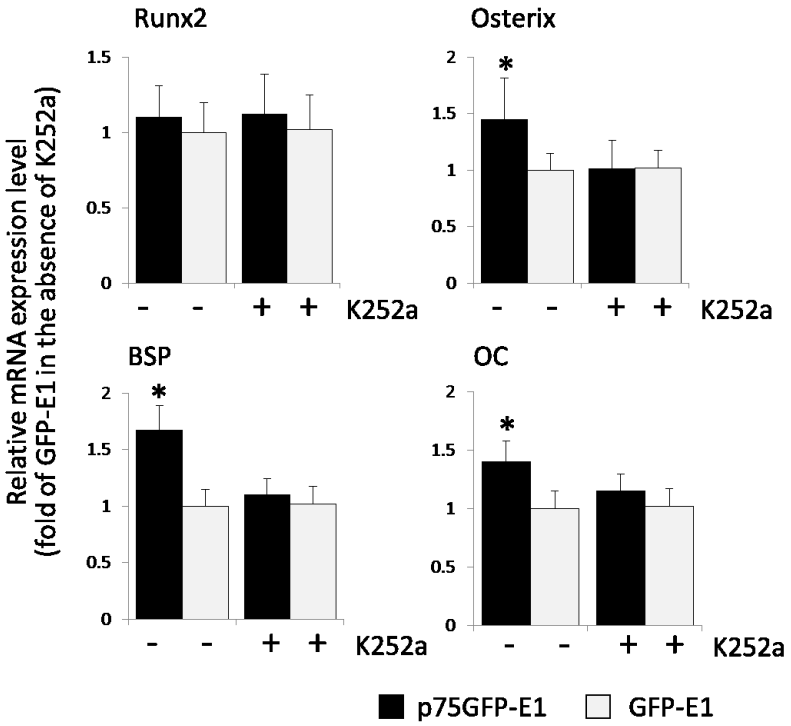

Supplemental data

Effect of K252a on p75^{NTR}-mediated mRNA expression of osteoblast transcription factors, Runx2 and OSX and the osteoblast markers, BSP and OC.

Cells were cultured in growth medium until confluent, and then cultured in osteogenic induction medium in the absence or presence of K252a (30 nM) for 12 d before real time RT-PCR was performed. Data are the mean ± S.D. (n = 3). *P < 0.05 compared with each GFP-E1.